Available online at www.sciencedirect.com
SCIENCE DIRECT®
Marine Geology 203 (2004) 261–268
MARINE GEOLOGY
INTERNATIONAL JOURNAL OF MARINE GEOLOGY, GEOCHEMISTRY AND GEOPHYSICS
www.elsevier.com/locate/margeo

Submarine landslides of San Pedro Escarpment, southwest of Long Beach, California

Robert G. Bohannon*, James V. Gardner

United States Geological Survey, Mailstop 980, P.O.Box 25046, Federal Center, Denver, CO 80225, USA

Accepted 5 September 2003

Abstract

The coastal infrastructure of the southern greater Los Angeles metropolitan area would be profoundly affected by a large tsunami. Submarine slope failures and active faults, either of which could have generated a tsunami, are known on the shelf and slope near Long Beach. Large slope failures are present on the San Pedro Escarpment and on the basin slope adjacent to the San Pedro shelf. The southeastern part of the escarpment has had a long history of slope failure. The most recent failure, the Palos Verdes slide, is over 4.5 km long, has been dated as 7500 years old, and involved over 0.34 km^3 of material, which now litters the adjacent basin floor. Other, smaller, deposits from nearby failures are also present, as are buried wedges of debris that indicate slope failures have occurred locally throughout the Holocene and much of the late Pleistocene. Slope failures have occurred in response to continual Quaternary uplift of the Palos Verdes anticlinorium. The Palos Verdes slide could potentially have generated a failure-related tsunami with an amplitude in the range of 8–12 m because it apparently failed catastrophically, started in shallow water, evolved on low-drag bedding planes, had a long slide path, and involved high-strength lithified material.

Keywords: tsunamis; California; submarine environment; mass movements; avalanches; seismic methods; Holocene; earthquakes

1. Introduction

The city of Long Beach, California's fifth largest city (Fig. 1), is built in an area of rapid geologic changes that are associated with a modern period of mountain building known locally as the Pasadenan orogeny (Wright, 1991). The greater Long Beach area includes one of the largest commercial centers in the United States, including the two busiest container ports in the country and several major offshore and onshore oil fields. With so much shoreline infrastructure within a few meters of sea level, Long Beach would be profoundly affected by a large tsunami.

The historic record suggests that large tsunamis have been rare in California primarily because those generated at subduction zones along the Pacific rim are commonly reduced to small waves by the time they reach the California coastline (McCulloch, 1985). The greater Long Beach area is further protected from the usual easterly travel

* Corresponding author. Tel.: +1-303-236-1235; Fax: +1-303-236-5690.
E-mail address: bbohannon@usgs.gov (R.G. Bohannon).

0025-3227/03/$ – see front matter © 2003 Elsevier B.V. All rights reserved.
doi:10.1016/S0025-3227(03)00309-8

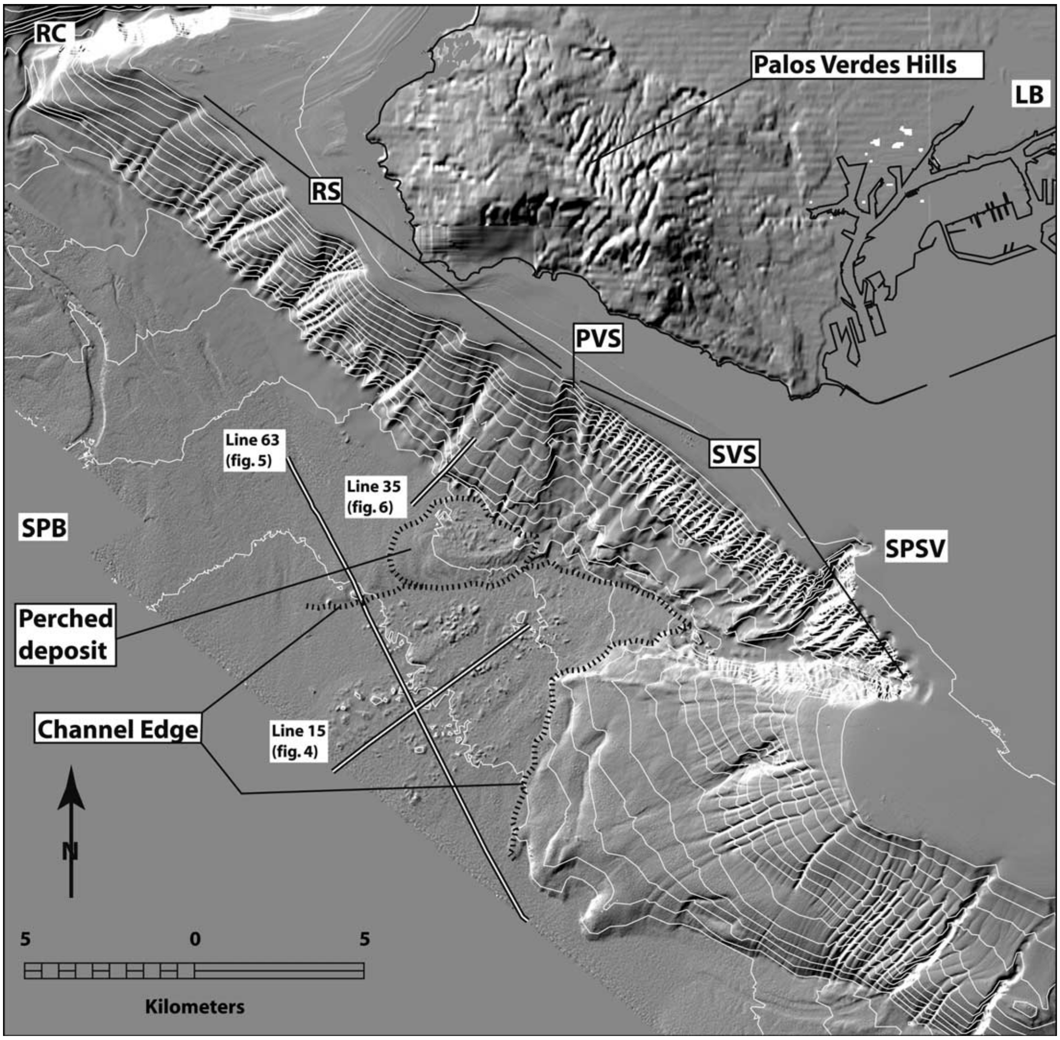

Fig. 1. Shaded relief map of the study area showing locations of various described features (contour interval = 50 m). Abbreviations: RC, Redondo Canyon; RS, Redondo segment of San Pedro Escarpment; SVS, Sea Valley segment of San Pedro Escarpment; SPSV, San Pedro Sea Valley; PVS, Palos Verdes scar; LSS, Lower slope slump; SPB, San Pedro Basin; LB, Long Beach.

directions of most distantly generated tsunamis by the Palos Verdes Peninsula and the Channel Islands. However, the Pasadenan orogeny is noted for its seismicity (Wright, 1991) and for localized areas of rapid uplift that resulted in steep and unstable slopes (e.g. Ehlig, 1987). Much of the modern tectonic activity occurs offshore, so there is a significant potential for local tsunamigenesis. Locally generated tsunamis can be large and very destructive (McCulloch, 1985). A recent example is the 1998 Papua New Guinea tsunami that was 15 m high, resulted in 2200 casualties, and was probably generated by a large submarine slide (Kawata et al., 1999; Tappin et al., 1999; Tappin et al., 2001).

This paper is focused on young submarine mass failures that have occurred offshore of the Long Beach area (Fig. 1). We examine part of the San Pedro Escarpment where morphologic features typical of large submarine slope failures are present. The escarpment can be divided into two segments. The northwest segment is the steep, linear basin slope southwest of the Palos Verdes Peninsula, which is marked by arcuate headwall scarps and steep-walled linear channels (Fig. 1). The southeast segment is the eastern extension of the escarpment where it becomes the northern wall of the San Pedro Sea Valley.

2. Data

The entire area was mapped with high-resolution multibeam sonar (MBES) (Gardner et al., 1999; Gardner and Mayer, 1998). The San Pedro shelf was mapped with a 300-kHz Kongsberg Simrad EM3000D system and the slope and proximal basin were mapped with a 30-kHz Kongsberg Simrad EM300 system. These data provide very accurate bathymetry for the area. Navigation for both surveys used differential-GPS-aided inertial navigation systems. Positions are accurate to within $< \pm 1$ m. The spatial resolution of the HRMB data is 4 m for shelf depths and 8 m for basin-slope depths.

High-resolution multichannel seismic data and Huntec deep-tow boomer profiles were collected on a grid of tracklines spaced at 2–4 km (Normark et al., 1999a; Normark et al., 1999b). These systems imaged the internal structure of the shelf and basin slope and help constrain our interpretations of the failures. High-resolution Huntec DTS boomer data produce images of the upper few tens of milliseconds of strata with a resolution of better than 0.5 ms (0.4 m).

3. San Pedro Escarpment

The San Pedro Escarpment is a 25-km-long linear basin slope that flanks the southwestern edge of the Palos Verdes uplift between San Pedro Sea Valley and Redondo Canyon (Fig. 1). The escarpment is oriented N27°W with slopes that range from 11.5° to 17° between water depths of 75–750 m. The escarpment is the dip slope of the southern limb of the Palos Verdes anticlinorium (Dibblee, 1999). The change in slope at the base of the escarpment is abrupt along its entire length, decreasing from $>10°$ to $<2°$ (Fig. 2). The surface trace of the San Pedro Escarpment Fault (Nardin and Henyey, 1978) is coincident with the base of the escarpment.

We call the southeastern half of the San Pedro

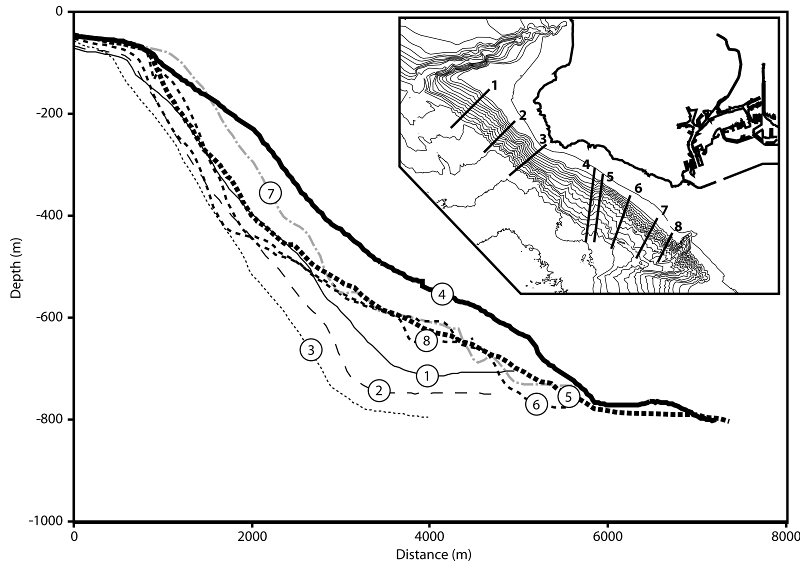

Fig. 2. Slope profiles of San Pedro Escarpment. Compare profile 4 (heavy solid line), drawn at edge of Redondo segment parallel to PVS, to profile 5 (heavy dashed line), drawn down axis of PVS. This comparison helps conceptualize the amount of material removed during PVS debris avalanche.

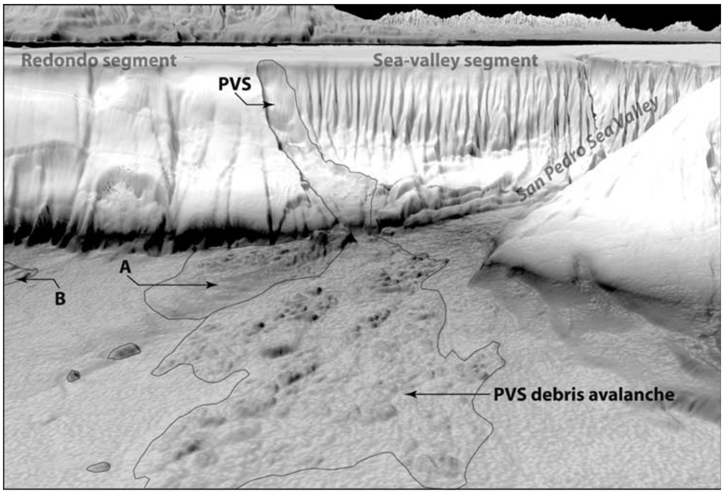

Fig. 3. Perspective view looking north–northeast at San Pedro Escarpment and San Pedro Sea Valley. Vertical exaggeration 5×. PVS marks top of valley failure scar that divides Redondo segment (to its left) and SVS (to its right) of San Pedro Escarpment. Numerous gullies of SVS contrast with much smoother, lobate sections of Redondo segment. Foreground shows high-relief seafloor of PVS debris-avalanche deposit contained within broad, shallow channel downslope from San Pedro Sea Valley. (A) perched debris-flow deposit visible to left (northwest) and above channel near base of escarpment; (B) another debris-flow deposit from an earlier episode of sliding or slumping on the escarpment.

Escarpment the sea-valley segment (SVS) and the northwestern half the Redondo segment (RS). The SVS is very straight and is characterized by abundant linear channels that incise its steep upper slope. The lower slope is smooth and gentle compared to the upper slope (Fig. 3). The SVS is eroded back 0.5 km to the northeast relative to the Redondo segment. The SVS is an area of submarine landslide features (Hampton et al., 2002; Hampton et al., 1996). The Redondo segment has a series of lobate ridges that are each 2.5–3.5 km wide and separated by deep, narrow, linear channels.

The largest individual failure scar in the area, herein called the Palos Verdes scar (PVS), separates the Redondo and the SVS (Fig. 3). The elongate scar is oriented north–south and has a pronounced arcuate headwall (Fig. 3). The PVS extends from the shelf break at about 70 m depth to the base of the basin slope at about 780 m. The PVS is 2 km wide at its base, 4.6 km long, and incises as much as 70 m into the escarpment (Fig. 2, profiles 4 and 5). The floor of the PVS includes large blocks up to 4 m high and 200 m in plan dimension. The volume of the PVS is 0.34–0.72 km^3, suggesting this much material was removed.

The PVS debouches into a broad, shallow channel on the floor of San Pedro Basin (Fig. 3). The channel is about 15 m deep and is 3.5–5.5 km wide below the PVS. East of the PVS, the channel narrows into the steep-walled canyon of San Pedro Sea Valley (Fig. 3). Below the mouth of the PVS, the floor of this channel is littered with debris-avalanche blocks, several of which are as high as 15 m and hundreds of meters long (Fig. 3). Runout distances of the blocks are as great as 8 km from the base of the escarpment. Huntec profiles show that the blocks in the broad valley are encased in an acoustically transparent matrix. The blocks and matrix rest on an older hummocky surface (Fig. 4). Roughly 32 km^2 of the channel floor is covered by the debris-avalanche deposits. If all the blocks were derived from the PVS, then one might expect the debris-avalanche deposits to be 10.6–22.5 m thick, given the volume estimate of the scar. The transparent deposit is 0.02 s (15+ m) thick at its thickest point along one of the Huntec profiles and it probably averages 10–12 m of thickness (Fig. 4), reflecting a similar volume to the PVS.

Other similar, but less extensive, debris-flow deposits are apparent on the basin floor to the west

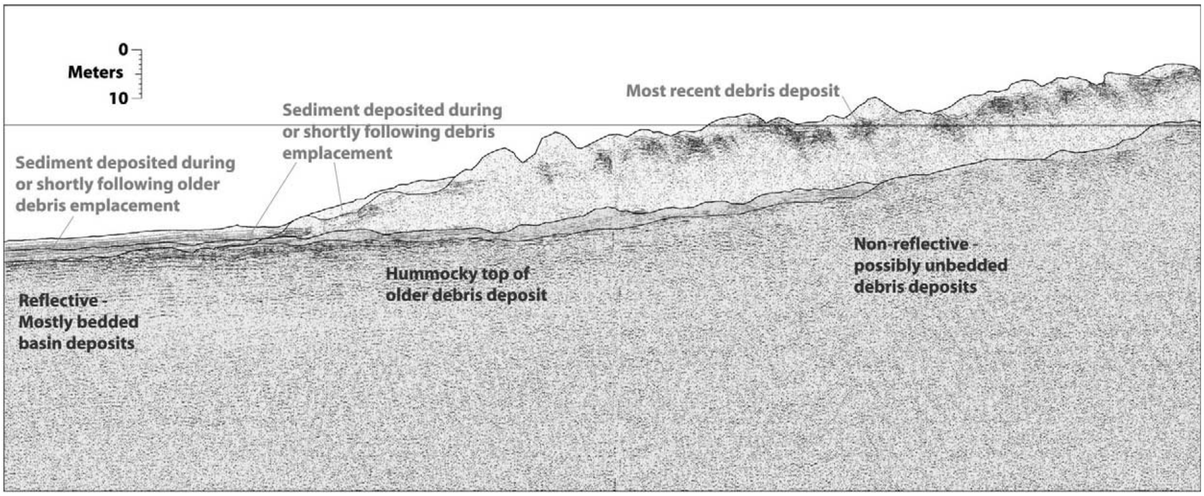

Fig. 4. Segment of Huntec, deep-tow boomer profile 198SC 15 through southwest edge of PVS debris-avalanche deposit. We use a velocity of 1500 m/s to approximate thickness of reflections in shallow part of profile. See Fig. 1 for location.

and northwest of the mouth of the PVS. One of these is 8 km^2 in plan view and averages 0.035 s (26+ m) in thickness. This large deposit (Fig. 1 and 'A' on Fig. 3) is perched several meters above the north wall of the broad channel that contains the PVS debris-avalanche deposit. Another smaller debris deposit ('B' on Fig. 3) is present about 3 km to the northwest. These smaller debris-flow deposits all lie near the base of the escarpment adjacent to the numerous small failure scars on its lower basin slopes.

Multichannel-seismic data suggest that numerous thick and acoustically unstratified deposits lie buried in this part of the basin. The southeast end of line 198SC-63 (Fig. 5) shows that the upper 600 m of basin fill, directly beneath the PVS debris-avalanche deposit, contains several thick (0.1 s or ~75 m) acoustically transparent lenses that are interpreted as landslide debris. Zones of disrupted reflectivity are common in the seismic data, suggesting the presence of numerous thinner landslide deposits. The multichannel data suggest that allochthonous deposits are a common component of the local late Quaternary and Holocene sedimentary record. The acoustic transparency of the allochthonous deposits contrasts with the surrounding highly reflective deposits that occur elsewhere in the basin (e.g. Fig. 5).

The age of the PVS debris-avalanche deposit has been tentatively constrained by Normark et al. (2004). Their radiocarbon dates from piston-core samples obtained near the distal toe of the deposit indicate that it is about 7500 years old. Normark et al. (2004) sampled planktonic foraminifera from a layer thought to directly underlie the deposit.

4. Discussion and conclusions

There is ample evidence that the SVS of the San Pedro Escarpment and the basin slope south of San Pedro Sea Valley have been the source of both large and small slope failures throughout much of the late Quaternary. The evidence presented here is consistent with the conclusion that many of these failures, especially the PVS, resulted in large debris avalanches. Although it is not known if these failures resulted in a tsunami, their scales are such that they potentially could have. We recognize that fault displacements might also be an important local source of tsunamis and that earthquakes might trigger slope failure, but a discussion of the complex local pattern of active faults and earthquakes and their relation to tsunamigenesis is beyond the scope of this paper.

The SVS of the San Pedro Escarpment is a region where a large amount of slope material

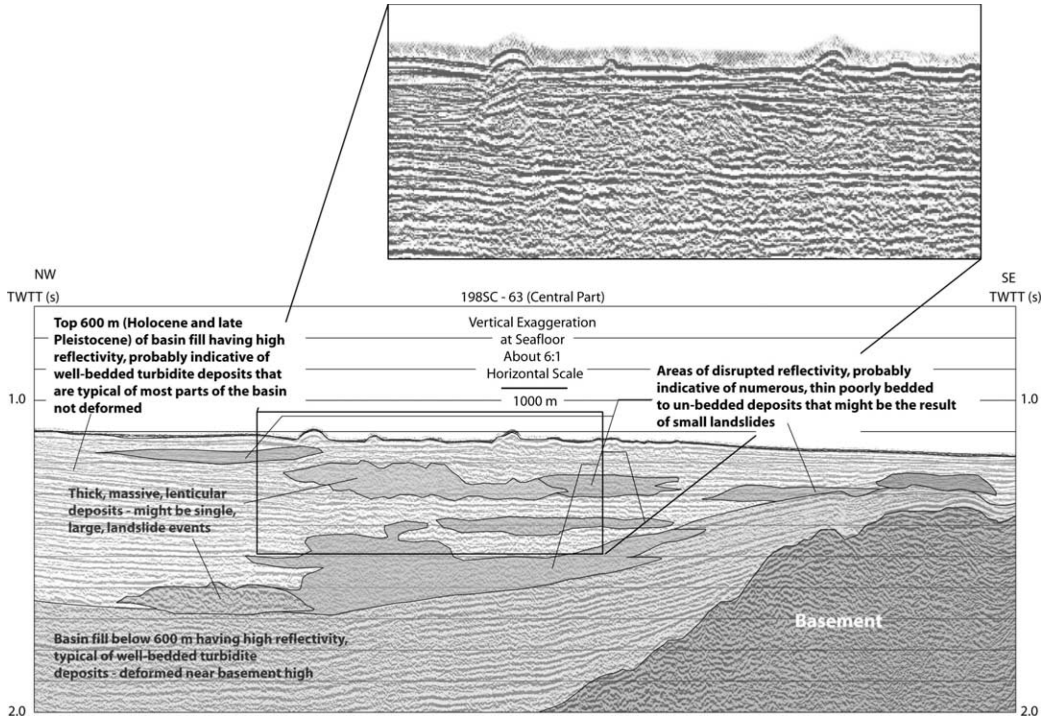

Fig. 5. Segment of migrated multi-channel seismic profile 198SC-63 with interpretation. See Fig. 1 for location. Inset shows detail of one thick, massive, lense that might be single-event mass-flow deposit buried beneath PVS debris-avalanche deposit.

has been removed by landsliding. In contrast, most of the bedded sedimentary rocks underlying the slope of the Redondo segment are still in place (Fig. 6). Consequently, the Redondo segment would appear to have a higher potential for future failures than the SVS. Failure appears to have occurred on bedding planes in lithified rocks, probably the Miocene Monterey Formation or possibly early Pliocene Repetto Formation (e.g. Dibblee, 1999). These bedded rocks form dip slopes on the south flank of the Palos Verdes anticlinorium (Fig. 6). The anticlinorium is active and elevated marine terraces suggest local uplift rates of 0.24–0.82 m/ky during the past 0.45–1.50 my (Ward and Valensise, 1994). The failures were probably set up as the slopes became tectonically oversteepened and gravitational stress exceeded the failure strength of the bedded rocks. Local earthquakes, such as the 1979 (M_L 5.2) and 1989 (M_L 5.0) Malibu earthquakes on the Santa Monica shelf (Hauksson and Saldivar, 1989), not only contribute to local uplifts but could provide a viable triggering mechanism for the failures, although we note the conclusions of Locat et al. (this volume) stability analysis that an earthquake with a magnitude of around 7 may be needed to trigger the slide.

There are theoretical reasons to suspect that large failures such as the PVS might have been accompanied by a tsunami (e.g. Ward, 2001) and it is possible to estimate the potential amplitude of the wave that was produced (Fig. 7), based on analyses of artificial-wave-machine data (Watts, 1998). Once triggered, a slide that begins at sea level, proceeds catastrophically downslope (negligible retardation due to friction) so it is assumed to convert all of its potential energy (E_p) to kinetic energy (E_k).

$$E_p = mgh \tag{1}$$

where m is the mass of the slide, g is gravitational acceleration, and h is the drop in height of the center of mass. Our data allow us to quantify the mass of the PVS debris-avalanche deposit if:

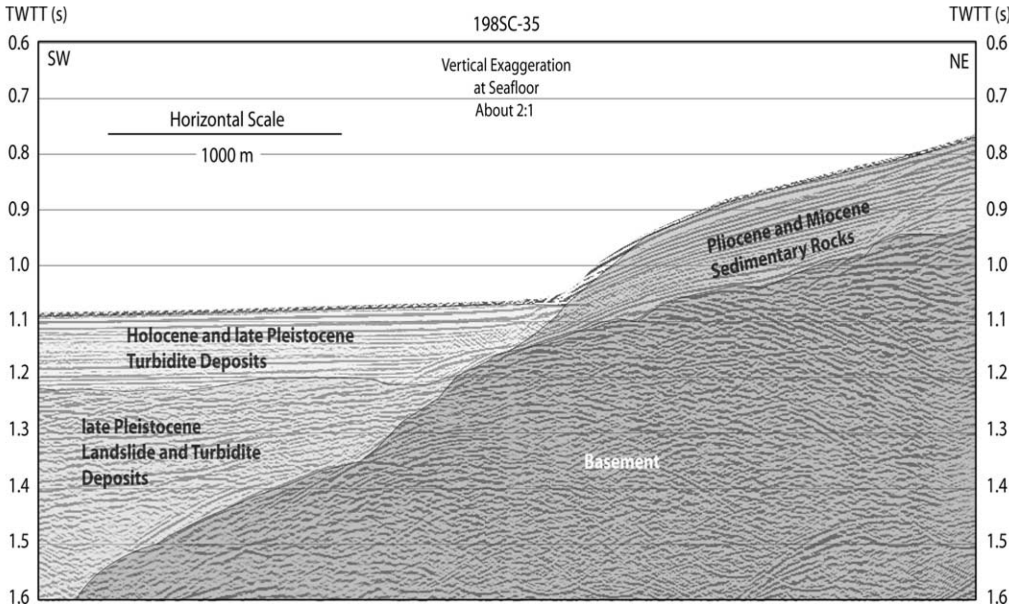

Fig. 6. Segment of migrated multi-channel seismic profile 198SC-35 with interpretation. See Fig. 1 for location. View shows cross-section of Redondo segment of San Pedro Escarpment that is perpendicular to slope.

$$m = (\rho_s - \rho_o)V = (\rho_s - \rho_o)wtl \quad (2)$$

because we know its width (w), thickness (t), and length (l), the density of sea water (ρ_o), and we can estimate the average slide density (ρ_s). Tsunami wave energy (E_t) can be related to E_p following Watts (1998) as:

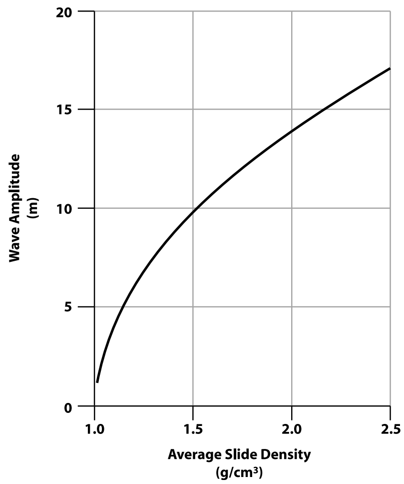

Fig. 7. Plot of Eq. 4 from text showing predicted tsunami wave amplitude for a range of possible average slide densities.

$$E_t = \eta\ E_p = \rho_o\ gw\lambda a^2 \quad (3)$$

where λ is tsunami wavelength (assumed to be $\approx$10 000 m), a is tsunami amplitude measured from sea level to crest, and η is a dimensionless factor of efficiency. Combining Eqs. 1–3 and solving for amplitude yields:

$$a = \sqrt{\frac{\eta(\rho_s - \rho_o)tlh}{\rho_o \lambda}} \quad (4)$$

The results of Eq. 4 plotted over a range of average slide densities, where η is assumed to be 2% (Wiegel), $t = 70$ m, $h = 350$ m, and l is 4000 m. These values, measured from our analysis of the PVS data, suggest that reasonable estimates of tsunami amplitude from the PVS range from 8 to 12 m, since the slide density would be between that of sea water and intact rock ($\sim$1.5 g/cm^3). This tsunami height estimate is for the immediate source area and does not take into account attenuation with distance from the source. Also, the estimate is based on a rigid-slide-mass assumption, which was probably not the case. Attenuation and a non-rigid slide would reduce the wave height. The tsunami-height estimate calculated is at the lower end of that calculated by Locat et al. (this volume).

Tsunami deposits are known from the west coast of the US (e.g. Atwater et al., 1995) and they provide a record of large prehistorical waves, although none have been described from the Long Beach area. An 8–12-m wave might not leave much of a geologic record and subsequent urbanization would make it hard to find any evidence that may have once existed.

Acknowledgements

We would like to thank Phil Watts for helping us understand the mechanics of tsunami generation during submarine landsliding. This paper was helped by reviews from Phil Watts, Mark Legg, and George Ferentinos.

References

Atwater, B.F. et al., 1995. Summary of coastal geologic evidence for past great earthquakes at the Cascadia subduction zone. Earthq. Spectra 11, 1–18.

Dibblee, T.W. Jr., 1999. Geologic Map of the Palos Verdes Peninsula and Vicinity, Redondo Beach, Torrance, and San Pedro Quadrangles, Los Angeles County, California. Dibblee Geological Foundation.

Ehlig, P.L., 1987. Portuguese Bend landslide complex, Southern California. In: Hill, M.L. (Ed.), Centennial Field Guide, Cordilleran Section of the Geological Society of America. Geological Society of America, Boulder, CO, pp. 179–184.

Gardner, J.V., Hughes Clarke, J.E., Mayer, L.A., 1999. Cruise report; RV Coastal Surveyor cruise C1-99; Multibeam Mapping of the Long Beach California Continental Shelf; April 12, through May 19, 1999. OF 99-0360, US Geological Survey, Reston, 43 pp.

Gardner, J.V., Mayer, L.A., 1998. Cruise report; RV Ocean Alert cruise A2-98-SC; Mapping the Southern California Continental Margin; March 26 through April 11, 1998; San Diego to Long Beach, California. OF 98-0475, US Geological Survey, Reston, 26 pp.

Hampton, M.A., Karl, H.A., Murray, C.J., 2002. Acoustic profiles and images of the Palos Verdes margin: Implications concerning deposition from the White's Point outfall. Cont. Shelf Res. 22, 841–857.

Hampton, M.A., Lee, H.J., Locat, J., 1996. Submarine landslides. Rev. Geophys. 34, 33–59.

Hauksson, E., Saldivar, G.V., 1989. Seismicity and active compressional tectonics in Santa Monica Bay, Southern California, Special section on Whittier Narrows earthquake. J. Geophys. Res. 94, 9591–9606.

Kawata, Y. et al., 1999. Tsunami in Papua New Guinea was as intense as first thought. Eos, Trans. Am. Geophys. Union 80, 101.

Locat, J., Lee, H.J., Locat, P., Imran, J., this volume. Numerical analysis of the mobility of the Palos Verdes debris avalanche, California, and its implication for the generation of tsunamis.

McCulloch, D.S., 1985. Evaluating earthquake hazards in the Los Angeles region – An earth science perspective. US Geol. Surv. Prof. Pap. 1360, US Dept. of Interior, Washington, DC.

Nardin, T.R., Henyey, T.L., 1978. Pliocene–Pleistocene diastrophism of Santa Monica and San Pedro shelves, California continental borderland. AAPG Bull. 62, 247–272.

Normark, W.R., et al., 1999a. Cruise report for A1-98-SC Southern California Earthquake Hazards Project. OF 99-0152, US Geological Survey, Reston, 60 pp.

Normark, W.R., McGann, M., Sliter, R.W., 2004. Age of Palos Verdes submarine debris avalanche, southern California. Mar. Geol. 203, doi: 10.1016/S0025-3227(03)00308-6, this issue.

Normark, W.R., et al., 1999b. Cruise report for 01-99-SC; Southern California Earthquake Hazards Project. OF 99-0560, US Geological Survey, Reston, 60 pp.

Tappin, D.R., Matsumoto, T., and shipboard scientists, 1999. Offshore geological investigation of the July 1998 Sissano tsunami, Papua New Guinea. EOS, Trans. Am. Geophys. Union, 80(30), 329.

Tappin, D.R., Watts, P., McMurtry, G.M., Lafoy, Y., Matsumoto, T., 2001. The Sissano, Papua New Guinea tsunami of July 1998 – Offshore evidence on the source mechanism. Mar. Geol. 175, 1–23.

Ward, S.N., 2001. Landslide tsunami. J. Geophys. Res. 106, 11201–11215.

Ward, S.N., Valensise, G., 1994. The Palos Verdes terraces, California; Bathtub rings from a buried reverse fault. J. Geophys. Res. 99, 4485–4494.

Watts, P., 1998. Wavemaker curves for tsunamis generated by underwater landslides. J. Waterway Port Coast. Ocean Eng. 124, 127–137.

Wiegel, R.L., 1955. Laboratory studies of gravity waves generated by the movement of a submarine body. Trans. Am. Geophys. Union 36, 759–774.

Wright, T.L., 1991. Structural geology and tectonic evolution of the Los Angeles Basin, California. In: Biddle, K.T. (Ed.), Active Margin Basins. Mem. Am. Assoc. Pet. Geol. 52, 35–134.